Direct Conversion of Human Endothelial Cells Into Liver Cancer-Forming Cells Using Nonintegrative Episomal Vectors

Takeshi Goya,[1,2] Kenichi Horisawa,[1] Miyako Udono,[1] Yasuyuki Ohkawa,[3] Yoshihiro Ogawa,[2] Sayaka Sekiya,[1] and Atsushi Suzuki[1]

Liver cancer is an aggressive cancer associated with a poor prognosis. Development of therapeutic strategies for liver cancer requires fundamental research using suitable experimental models. Recent progress in direct reprogramming technology has enabled the generation of many types of cells that are difficult to obtain and provide a cellular resource in experimental models of human diseases. In this study, we aimed to establish a simple one-step method for inducing cells that can form malignant human liver tumors directly from healthy endothelial cells using nonintegrating episomal vectors. To screen for factors capable of inducing liver cancer-forming cells (LCCs), we selected nine genes and one short hairpin RNA that suppresses tumor protein p53 (*TP53*) expression and introduced them into human umbilical vein endothelial cells (HUVECs), using episomal vectors. To identify the essential factors, we examined the effect of changing the amounts and withdrawing individual factors. We then analyzed the proliferation, gene and protein expression, morphologic and chromosomal abnormality, transcriptome, and tumor formation ability of the induced cells. We found that a set of six factors, forkhead box A3 (FOXA3), hepatocyte nuclear factor homeobox 1A (HNF1A), HNF1B, lin-28 homolog B (LIN28B), MYCL proto-oncogene, bHLH transcription factor (L-MYC), and Kruppel-like factor 5 (KLF5), induced direct conversion of HUVECs into LCCs. The gene expression profile of these induced LCCs (iLCCs) was similar to that of human liver cancer cells, and these cells effectively formed tumors that resembled human combined hepatocellular–cholangiocarcinoma following transplantation into immunodeficient mice. *Conclusion:* We succeeded in the direct induction of iLCCs from HUVECs by using nonintegrating episomal vectors. iLCCs generated from patients with cancer and healthy volunteers will be useful for further advancements in cancer research and for developing methods for the diagnosis, treatment, and prognosis of liver cancer. (*Hepatology Communications* 2022;6:1725-1740).

Liver cancer is the fourth most lethal malignancy worldwide[(1)] and remains a major health problem. Elucidating the precise mechanism of tumor initiation and progression is necessary to develop novel therapies for liver cancer, and appropriate experimental models are important for such studies. Therefore, several experimental models, such as those chemically induced, xenograft modified, and genetically modified, have been developed.[(2)] In chemically induced models, administration of a chemical reagent promotes inflammation followed by fibrosis and eventually leads to liver cancer. The advantage of chemically induced mouse models is their similarity to human liver cancer in the context of liver inflammation and fibrosis. However, chemically induced models incompletely mimic human cancers because the

Abbreviations: 6MIX, mixture of 6 plasmids; 10MIX, mixture of all plasmids; AFP, α-fetoprotein; ALB, albumin; BLIMP1, PR domain containing 1with ZNF domain; C5, complement C5; CCC, cholangiocellular carcinoma; CCNA2, cyclin A2; CCNB1, cyclin B1; CCNB2, cyclin B2; CCND1, cyclin D1; CCND2, cyclin D2; CD, clusters of differentiation; CDH1, cadherin1; CDH5, cadherin5; CDK1, cyclin dependent kinase 1; CEACAM5, CEA cell adhesion molecule 5; CHC, combined hepatocellular–cholangiocarcinoma; CK19, cytokeratin 19; c-Myc, MYC proto-oncogene, bHLH transcription factor; DAPI, 4′,6-diamidino-2-phenylindole; EBNA1, Epstein-Barr nuclear antigen 1; EPCAM, epithelial cell adhesion molecule; ERBB2, erb-b2 receptor tyrosine kinase 2; ERK1, extracellular signal-regulated kinase 1; ERK2, extracellular signal-regulated kinase 2; FGF13, fibroblast growth factor 13; FGFR2, fibroblast growth factor receptor 2; FGFR3, fibroblast growth factor receptor 3; FOXA3, forkhead box A3; GATA4, GATA binding protein 4; GEO, Gene Expression Omnibus; GO, gene ontology; GPC3, glypican 3; H&E, hematoxylin-eosin; hAAT, human-specific α-1 antitrypsin; HCC, hepatocellular carcinoma; HepPC, hepatic progenitor cell; HMGA2, high mobility group AT-hook 2; HNF1A, hepatocyte nuclear factor homeobox 1A; HNF1B, hepatocyte nuclear factor homeobox 1B; HNF4A, hepatocyte nuclear factor 4 alpha; HNF6, One Cut Homeobox 1; HUVEC, human umbilical vein endothelial cell; iHepPC, induced hepatic progenitor cell; iLCC, induced liver cancer-forming cell; iPSC, induced pluripotent stem cell; KLF5, Kruppel-like factor 5; LCC, liver cancer-forming cell; let-7, lethal-7; Lin28b, lin-28 homolog B; L-MYC, MYCL Proto-Oncogene, BHLH Transcription Factor; MAPKK, mitogen-activated protein kinase kinase; NOS3, nitric oxide synthase 3; NOTCH3, notch receptor 3; p, plasmid; PAK1, p21 (RAC1) activated kinase 1; PCNA, proliferating cell nuclear antigen; PECAM1, platelet/endothelial cell adhesion molecule 1; qPCR, quantitative polymerase chain reaction; RAS, Ras-like protein; shRNA, short hairpin RNA; SOX9, SRY-box transcription factor 9; SV40LT, SV40 large T antigen; TEAD2, TEA domain transcription factor 2;

reagents used in these models are never administered to humans and there are biological differences between humans and mice. Xenograft models are expected to better reflect the features of the original human cancer. Because of interpatient and intratumoral heterogeneity, elucidation of the general mechanism in all liver cancers requires collection of a vast number of human samples. Hence, xenograft models require an enormous amount of time, cost, and labor. In genetically modified models, liver cancer is induced by transduction of oncogenes and recapitulates the molecular biological mechanisms. However, complete recapitulation of mutations in human liver cancer is challenging because human liver cancers carry multiple mutations. Thus, conventional mouse models have certain limitations. Although xenograft mouse models have the advantage of using human cancer, they are not easily available for the reasons mentioned above. Hence, more convenient and cost-effective experimental models using human cells are needed for research on human liver cancer.

Hepatocellular carcinoma (HCC) constitutes the majority of liver cancers. Although the cell of origin in liver cancers remains controversial, previous reports have demonstrated that hepatocytes and hepatic progenitor cells (HepPCs) transform into cancer cells.[3,4] Similarly, immature hepatocytes are assumed to generate hepatoblastoma, the most frequent primary liver cancer in childhood. Furthermore, cholangiocellular carcinoma (CCC) has been reported to be derived from hepatocytes or HepPCs in experimental murine models.[4] Taken together, these results suggest that HepPCs are involved in the development of primary liver tumor.[4]

We previously reported that a set of three transcription factors, forkhead box A3 (FOXA3), hepatocyte nuclear factor homeobox 1A (HNF1A), and HNF6, can induce direct conversion of human umbilical vein endothelial cells (HUVECs) into HepPCs. These induced HepPCs (iHepPCs) can give rise to both hepatocytes and cholangiocytes and reconstitute damaged liver tissues.[5] In this study, we attempted to develop a novel liver cancer model using direct reprogramming technology. Because cancer-related genes, such as MYC proto-oncogene, bHLH transcription factor (*c-Myc*)[6] and *p53*,[7] improve the reprogramming efficacy of induced pluripotent stem cells (iPSCs), we expected that oncogenes would have

TEAD4, TEA domain transcription factor 4; TERT, telomerase reverse transcriptase; TGFB1, transforming growth factor beta 1; TGFBR1, transforming Growth Factor Beta Receptor 1; TIAM1, TIAM Rac1-associated guanine nucleotide exchange factor 1; TP53, tumor protein p53.

Received June 15, 2021; accepted January 22, 2022.

Additional Supporting Information may be found at onlinelibrary.wiley.com/doi/10.1002/hep4.1911/suppinfo.

Supported in part by the Japan Society for the Promotion of Science Grants-in-Aid for Scientific Research (Grant Numbers: JP16H01850, JP17H05623, JP18H05102, JP19H01177, JP19H05267, JP20H05040, and JP21K19916 to Atsushi Suzuki), Core Research for Evolutional Science and Technology Program of the Japan Agency for Medical Research and Development (AMED) (JP16gm0510006 to Atsushi Suzuki), Program for Basic and Clinical Research on Hepatitis of AMED (JP17fk0210307 to Atsushi Suzuki), Research Center Network for Realization of Regenerative Medicine of AMED (JP20bm0704034 to Atsushi Suzuki), Takeda Science Foundation (to Atsushi Suzuki), Uehara Memorial Foundation (to Atsushi Suzuki), Mitsubishi Foundation (to Atsushi Suzuki), Kato Memorial Trust for Nambyo Research (to Atsushi Suzuki), and Princess Takamatsu Cancer Research Fund (to Atsushi Suzuki).

View this article online at wileyonlinelibrary.com.

DOI 10.1002/hep4.1911

Potential conflict of interest: Nothing to report.

ARTICLE INFORMATION:

From the [1]Division of Organogenesis and Regeneration, Medical Institute of Bioregulation, Kyushu University, Fukuoka, Japan; [2]Department of Medicine and Bioregulatory Science, Graduate School of Medical Sciences, Kyushu University, Fukuoka, Japan; [3]Division of Transcriptomics, Medical Institute of Bioregulation, Kyushu University, Fukuoka, Japan.

ADDRESS CORRESPONDENCE AND REPRINT REQUESTS TO:

Atsushi Suzuki, Ph.D.,
Division of Organogenesis and Regeneration
Medical Institute of Bioregulation
Kyushu University
3-1-1 Maidashi, Higashi-ku
Fukuoka 812-8582, Japan
E-mail: suzukicks@bioreg.kyushu-u.ac.jp
Tel.: +81-92-642-6449

the potential to cause the formation of cancers and improve reprogramming efficacy. In fact, Sun et al.[8] reported a liver cancer model using direct reprogramming technology. To understand the mechanism of cancer initiation, they established cancer organoids by using a two-step induction method. The first step involved the induction of expandable hepatocytes by overexpression of *FOXA3*, *HNF1A*, *HNF4A*, and SV40 large T antigen (*SV40LT*), which inactivates tumor protein p53 (*TP53*) and RB transcriptional corepressor 1 (*RB*), and the second step involved the acquisition of cancerous properties by additional overexpression of oncogenes, such as *c-MYC* and Ras-like protein (*RAS*). Cancer organoids could form liver cancer *in vivo*. Although further studies are necessary to assess whether these models mimic the process of human liver carcinogenesis, these organoids may be useful for the analysis of cancer initiation.

To facilitate the study of human liver cancers, we aimed to establish a simple one-step method of generating a liver cancer model using human cells that was advantageous in terms of reprogramming efficacy and speed. To this end, we modified the iHepPC induction method. First, we used episomal vectors instead of retroviral vectors. The vectors contained origin of plasmid replication and Epstein-Barr nuclear antigen 1 (*EBNA1*) sequences derived from the Epstein-Barr virus (EBV). These EBV-derived components enabled the vectors to remain in the nuclei of the host cells for a long time without genomic integration.[9] Viral vectors, such as retroviral and lentiviral vectors, are widely used in direct reprogramming. However, these vectors integrate into the host genome and have a possibility of causing carcinogenesis by insertional mutagenesis. In fact, hepatitis B virus and adeno-associated virus type 2 are associated with oncogenic insertional mutagenesis in HCC.[10,11] Furthermore, a hematopoietic tumor arose following retrovirus vector-based gene therapy as a consequence of insertional mutagenesis.[12] Therefore, we selected episomal vectors to avoid unintentional carcinogenesis caused by insertional mutagenesis. Second, we defined six genes for the induction of liver cancer-forming cells (LCCs) by screening candidate genes. Our defined gene set directly induced the conversion of HUVECs into cells with liver cancer properties. The induced cells acquired gene expression patterns similar to those of human liver cancer cell lines and formed liver cancer *in vivo*. Thus, these induced cells were designated "induced liver cancer-forming cells" (iLCCs). iLCCs may contribute to the development of basic research and therapeutic strategies for liver cancer.

Materials and Methods

MICE

Eight female and four male nonobese diabetic (NOD)/severe combined immunodeficiency (SCID)/gamma (NSG) (NOD.Cg-*Prkdc*^{scid}*Il2rg*^{tm1Wjl}/SzJ) mice (3 weeks old; Charles River Laboratories) were used in this study. Mice were housed in groups of two to four per cage in a 12-hour light/dark cycle (08:00AM-8:00PM light; 8:00PM-08:00AM dark), with controlled room temperature (22°C ± 4°C) and relative humidity (60%). The experiments were approved by the Kyushu University Animal Experiment Committee. All animals received humane care, and studies using animals were performed in accordance with the institutional guidelines.

GENERATION OF ILCCS WITH EPISOMAL VECTORS

HUVECs (PromoCell, Cat. No. C-12203) supplied from pooled donors (from up to four different umbilical cords) were purchased and cultured in HUVEC medium (1:1 mixture of Medium 200 [Thermo Fisher Scientific], supplemented with low serum growth supplement [Thermo Fisher Scientific], and FibroLife S2 Comp Kit [Kurabo]) with 1 μM A83-01 (Tocris), 5 μM Y-27632 (Wako), and 3 μM CHIR99021 (Tocris) for 4 days at passage 2 after the thawing of cryopreserved HUVECs. Expression plasmid mixtures containing 1 μg of each expression plasmid and plasmid (p)CXWB-EBNA1 were electroporated into 6×10^5 HUVECs with the Neon Transfection System 100 μL Kit (Invitrogen) according to the manufacturer's instructions. The conditions used were 1,450 V, 10 milliseconds, and three pulses. After electroporation, the cells were plated in type I collagen-coated six-well plates (Iwaki) and grown in our hepato-medium composed of a 1:1 mixture of Dulbecco's modified Eagle's medium and F-12 (Nacalai Tesque), supplemented with 20% FibroLife S2 Comp Kit, 4% fetal bovine serum, 1 μg/mL insulin (Wako), 10^{-7} M dexamethasone (Sigma-Aldrich), 10 mM nicotinamide (Sigma-Aldrich), 2 mM L-glutamine (Nacalai Tesque), 50 μM β-mercaptoethanol (Nacalai Tesque),

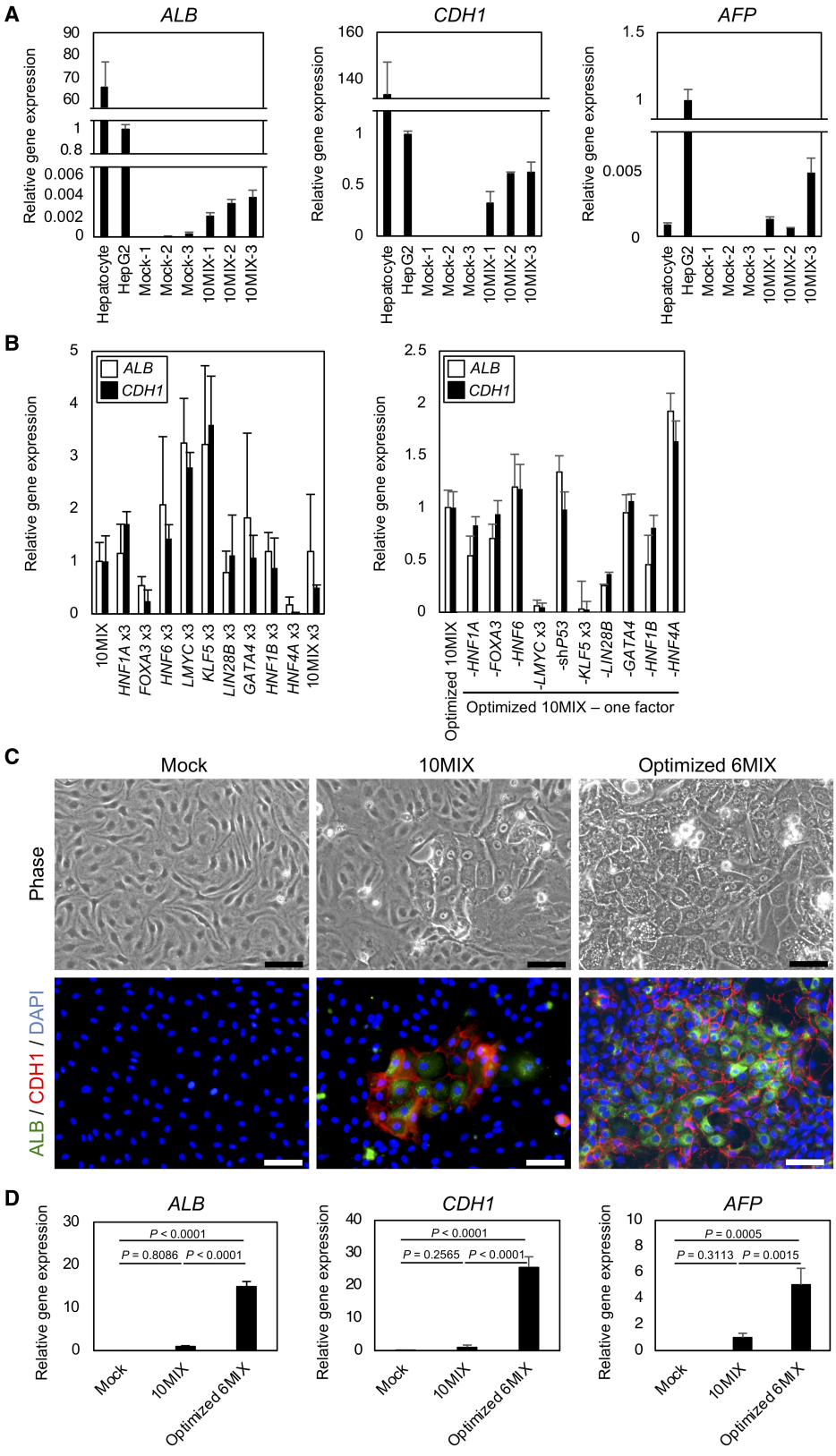
A
ALB
CDH1
AFP
Relative gene expression
Hepatocyte
HepG2
Mock-1
Mock-2
Mock-3
10MIX-1
10MIX-2
10MIX-3
B
ALB
CDH1
10MIX
HNF1A x3
FOXA3 x3
HNF6 x3
LMYC x3
KLF5 x3
LIN28B x3
GATA4 x3
HNF1B x3
HNF4A x3
10MIX x3
Optimized 10MIX
-HNF1A
-FOXA3
-HNF6
-LMYC x3
-shP53
-KLF5 x3
-LIN28B
-GATA4
-HNF1B
-HNF4A
Optimized 10MIX – one factor
C
Mock
10MIX
Optimized 6MIX
Phase
ALB / CDH1 / DAPI
D
ALB
CDH1
AFP
P < 0.0001
P = 0.8086
P < 0.0001
P = 0.2565
P < 0.0001
P = 0.0005
P = 0.3113
P = 0.0015
Mock
10MIX
Optimized 6MIX

FIG. 1. Screening for optimized factors to generate iLCCs from HUVECs. (A) qPCR analyses were performed on total RNA obtained from hepatocytes, HepG2 cells, mock-electroporated HUVECs, and 10MIX-induced cells. All data were normalized to the values from HepG2 cells, and the fold differences are shown. Data represent the mean ± SD; n = 3 independent experiments. (B) qPCR analyses were performed to examine the effect of changing the plasmid ratio (left; normalized with the values for 10MIX) and removing individual factors from the 10MIX pool (right; normalized with the values for optimized 10MIX). Fold differences are shown. Data represent the mean ± SD; n = 3 independent experiments. (C) Co-immunofluorescent staining of ALB and CDH1 was performed in mock-electroporated-, 10MIX-induced-, and optimized 6MIX-induced HUVECs. Representative fluorescence images and morphologies are shown. DNA was stained with DAPI. Scale bars, 50 μm. (D) qPCR analyses were performed on total RNA obtained from mock-electroporated-, 10MIX-induced-, and optimized 6MIX-induced HUVECs. All data were normalized to the values for HUVECs induced with 10MIX, and the fold differences are shown. Data represent the mean ± SD; n = 3 independent experiments. Statistical significance was analyzed using one-way analysis of variance followed by Tukey-Kramer test.

1 μM A83-01 (Tocris), 5 μM Y-27632 (Wako), and penicillin/streptomycin (Nacalai Tesque). At 40 days postelectroporation, the cells were passaged (split ratio 1:5) biweekly.

DATA AVAILABILITY STATEMENT

All data sets were deposited in the Gene Expression Omnibus (GEO) database under accession numbers GEO GSE168997 and GSE184539. Additional methods are available in the Supporting Information.

Results

OPTIMIZATION OF THE ONE-STEP INDUCTION METHOD

Candidate genes were selected for the induction of LCCs. Overexpression of lin-28 homolog B (*Lin28b*) has been reported to induce hepatoblastoma and HCC in the mouse liver.[13] That study reported high tumorigenesis efficacy of *Lin28b* (100% [9/9]). *Lin28b* has also been reported to play an important role in the maintenance of stem cell properties of hepatoblasts.[14] Therefore, we chose *LIN28B* as the key gene for the induction of LCCs. Although *c-MYC* is known to act as an oncogene, the tumorigenic efficiency of *c-Myc* overexpression was reported to be 58% (7/12)[15] in contrast to the higher efficiency of *Lin28b* overexpression. Moreover, *Lin28b* up-regulates *c-Myc* by inhibiting lethal-7 (*let-7*) maturation.[16] Another study reported that *c-Myc* induced *Lin28b* expression.[17] *LIN28B* and *c-MYC* may therefore comprise a positive feedback loop. Thus, we employed *LIN28B* but not *c-MYC*. In addition, we decided to perform Kruppel-like factor 5 (*KLF5*) overexpression, which is positively correlated with HCC malignancy,[18] and *TP53* inhibition, which is associated with poor prognosis in HCC.[19] Finally, our candidate gene pool consisted of the following 10 factors: iHepPC induction genes (*FOXA3*, *HNF1A*, and *HNF6*), an iHepPC promoting factor (*L-MYC*), other liver-associated genes (*HNF4A*, *HNF1B*, and GATA binding protein 4 [*GATA4*]), *KLF5*, TP53 short hairpin RNA (shRNA), and *LIN28B*. Furthermore, to increase the reprogramming efficiency, we added EBNA1 with an extra plasmid, pCXWB-EBNA1, which increased the efficiency of iPSC reprogramming.[9]

HUVECs are commercially available and easily obtained with little difference among the batch, which is a great advantage for replicating experiments for establishing the optimal reprogramming method. Moreover, HUVECs can be considered a good source of cells in the induction of direct cell-lineage reprogramming because HUVECs stably achieved direct induction of human hepatic and intestinal progenitor cells in our previous studies.[5,20] Thus, we selected HUVECs for the induction of LCCs. Episomal vectors expressing each gene and shRNA were prepared, and a mixture of all plasmids (referred to as 10MIX) was used to electroporate HUVECs. At 30 days postelectroporation with 10MIX, quantitative polymerase chain reaction (qPCR) analyses revealed induction of the expression of the hepatocyte/HepPC markers albumin (*ALB*), α-fetoprotein (*AFP*), and the epithelial cell marker cadherin1 (*CDH1*) (Fig. 1A). Next, to increase the reprogramming efficiency, we evaluated the stoichiometric effect because the stoichiometry of episomal vectors influences the reprogramming efficiency of iPSC induction.[21] We used 3 μg of one factor and 1 μg of other factors for electroporation and found that 3 times the amount of *L-MYC* or *KLF5* increased the expression of hepatocyte and epithelial cell marker genes (Fig. 1B). Furthermore, 3 times the amount of *KLF5* and *L-MYC* demonstrated an

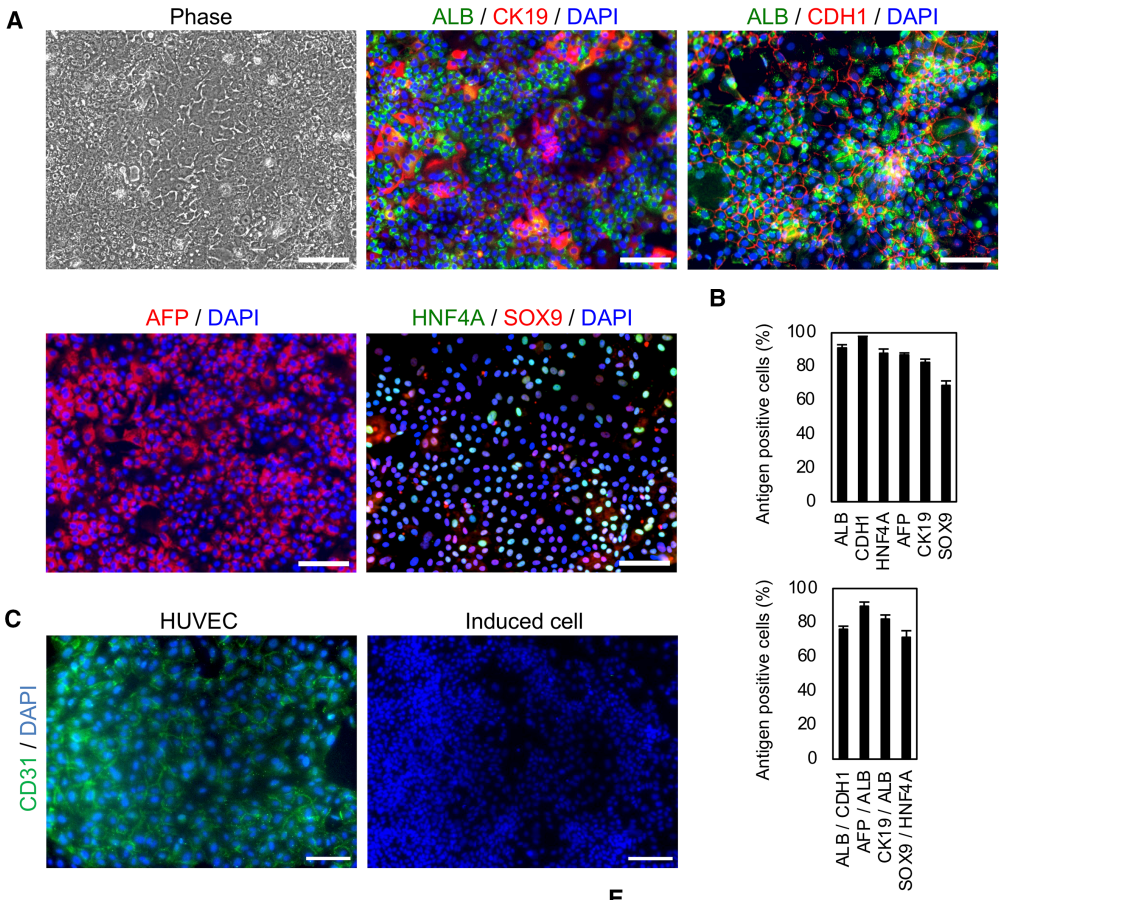

F

	Analysis of chromosome number				Karyotype analysis		
	Analyzed cell number	44	46	47	Analyzed cell number	46XY	46XY, chrb(6)(q22), chtb(11)(q13)
Induced cell-1	20 cells	0	19	1	8 cells	8	0
Induced cell-2	20 cells	1	17	2	8 cells	7	1

FIG. 2. Characterization of the induced cells. (A) Co-immunofluorescent staining of ALB with CK19, ALB with CDH1, AFP, and HNF4A with SOX9 was conducted in the induced cells. Representative fluorescence images and morphologies are shown. DNA was stained with DAPI. Scale bars, 50 μm. (B) Graphs show percentages of cells immunoreactive for each protein, and the graphs on the right show the percentages of ALB+ cells in CDH1+ cells, AFP+ cells in ALB+ cells, CK19+ cells in ALB+ cells, and SOX9+ cells in HNF4A+ cells, respectively. Data represent the mean ± SD; n = 3 independent experiments. (C) Immunofluorescent staining of CD31 was performed in HUVECs at passage 4 and the induced cells at passage 4. DNA was stained with DAPI. Scale bars, 100 μm. (D) Upper images show the morphologies of organoids formed from iHepPCs and the induced cells. Lower images show the H&E-stained sections of these organoids. Scale bars, 100 μm. (E) The dot plots show the nuclear-to-cytoplasmic ratio of each cell in the organoids formed from iHepPCs and three different induced cells. (F) The table shows the chromosome number and karyotype of cells in cultures of two different induced cells. Abbreviations: chrb, chromosome break; chtb, chromatid break.

additive effect in contrast to no additive effect of other factors (Supporting Fig. S1). Subsequently, we determined the essential factors by evaluating the expression of hepatocyte and epithelial cell marker genes. Withdrawing individual factors from the 10MIX indicated that *HNF6*, TP53 shRNA, *GATA4*, and *HNF4A* were not essential for the reprogramming (Fig. 1B). Finally, we determined 1 μg of *FOXA3*, *HNF1A*, *HNF1B*, and *LIN28B* and 3 μg of *L-MYC* and *KLF5* to be the optimized 6MIX. Nine days after electroporation of the optimized 6MIX, epithelial-like cell colonies emerged and the cells expressed hepatocyte and epithelial cell marker genes. The conversion efficiency was 0.138% as determined by counting the number of colonies (Supporting Fig. S2). We observed a larger number of ALB+ epithelial cells at 30 days postelectroporation with optimized 6MIX compared to that with 10MIX (Fig. 1C). qPCR analyses also revealed that the expression levels of hepatocyte and epithelial cell marker genes were significantly up-regulated in the optimized 6MIX-induced cells (Fig. 1D).

CHARACTERIZATION OF CELLS INDUCED WITH OPTIMIZED 6MIX

Immunofluorescence analyses revealed that the cells induced with optimized 6MIX expressed the hepatocyte-associated nuclear transcription factor HNF4A (87.7% ± 2.7%, n = 3), immature hepatocyte marker AFP (86.8% ± 1.3%, n = 3), and cholangiocyte markers cytokeratin 19 (CK19) (82.5% ± 1.9%, n = 3) and SRY-box transcription factor 9 (SOX9) (68.9% ± 2.6%, n = 3), in addition to ALB (90.8% ± 2.0%, n = 3) and CDH1 (97.2% ± 0.7%, n = 3) (Fig. 2A). Moreover, 76.0% ± 1.9% of CDH1+ cells expressed ALB, and 89.5% ± 2.6% of ALB+ cells expressed AFP, suggesting that the induced cells had immature hepatocyte properties. Furthermore, 82.0% ± 2.5% of ALB+ cells expressed CK19, and 71.4% ± 3.8% of HNF4A+ cells expressed SOX9 (Fig. 2B). Most of the induced cells expressed both hepatocyte and cholangiocyte markers. Thus, the induced cells were found to attain an undifferentiated state with hepatocyte and cholangiocyte properties.

In culture of the induced cells, any clusters of differentiation (CD)31-positive vascular endothelial cells were not observed (Fig 2C), suggesting that proliferating reprogrammed cells outcompeted unreprogrammed HUVECs. Furthermore, to test the cancerous properties of the induced cells *in vitro*, we performed a soft-agar colony formation assay, an organoid-forming assay, and karyotype analysis for induced cells. The induced cells did not show anchorage-independent growth ability in a soft-agar colony formation assay (Supporting Fig. S3). However, under three-dimensional culture conditions, induced cells formed morphologically abnormal organoids with an increased nucleus-to-cytoplasm ratio and enlarged pleomorphic nuclei compared with those formed from iHepPCs generated in our previous study (Fig. 2D,E).[5] Also, karyotype analysis showed that some cells contained in cultures of induced cells showed chromosomal instability (Fig. 2F; Supporting Fig. S4). These characteristics of the induced cells implied their cancerous phenotype in culture.

EVALUATION OF GENOMIC INSERTION AND EXPANSION IN LONG-TERM CULTURE

Next, we evaluated the genomic insertion of the episomal vectors by Southern blotting. In the induced cells, only a single band that was also detected in the episomal vector mix was detectable in contrast to multiple bands in HUVECs that contain random genomic insertions by *EBNA1*-expressing retrovirus vectors. These results showed that the vectors were

retained in the episome, and genomic insertions were not detectable (Fig. 3A). Moreover, the induced cells were maintained in long-term culture with proliferation and expression of *ALB*, *CDH1*, *AFP*, and *CK19* (Fig. 3B,C). Taken together, the induced cells could be considered as undifferentiated cells with hepatocyte and cholangiocyte properties and proliferate during long-term cultures without genomic integration.

GENE EXPRESSION PROFILE OF THE INDUCED CELLS

To assess the similarities between our induced cells and cancer cells, we investigated the global gene expression profile of our induced cells and that of human liver cancer cell lines, including HepG2 cells, Huh6 cells, Huh7 cells, and HuCCT1 cells, using a 3′ untranslated region sequencing (seq) method. Principal component analysis revealed that the expression signatures of the induced cells were similar to those of human cancer cell lines, indicating the malignant potential of the induced cells (Fig. 4A). To investigate the up-regulated genes in the induced cells, we extracted the commonly up-regulated genes in the induced cells and two cancer cell lines (hepatocyte lineage cancer cell line, HepG2; and/or cholangiocyte lineage cancer cell line, HuCCT1) compared to HUVECs. In the induced cells and HepG2 cells, the common up-regulated genes comprised genes related to protein synthesis, such as *ALB* and complement C5 (*C5*), and also genes, such as fibroblast growth factor receptor 3 (*FGFR3*) and erb-b2 receptor tyrosine kinase 2 (*ERBB2*), related to liver cancer malignancy.[22,23] Furthermore, the induced cells and both cancer cell lines commonly up-regulated the HCC-specific marker genes *AFP* and glypican 3 (*GPC3*),[24] immature marker genes epithelial cell adhesion molecule (*EPCAM*) and *SOX9* that are expressed in HCC and CCC,[25-28] and genes associated with epidermal growth factor (EGF) and FGF signaling that are activated in HCC and CCC.[29-32] The up-regulated genes common to the induced cells and HuCCT1 cells consisted of *FGFR2* (mutated in CCC[31]), TIAM Rac1-associated guanine nucleotide exchange factor 1 (*TIAM1*; associated with poor prognosis in HCC[33]), and p21 (RAC1) activated kinase 1 (*PAK1*; associated with HCC metastasis[34]) (Fig. 4B). Gene ontology (GO) analyses of these gene clusters revealed that the up-regulated genes common to the induced cells and HepG2 cells were significantly enriched in genes related to hepatic functions associated with the GO terms "cholesterol metabolism" and "glucogenesis." In addition, GO terms associated with proliferation and carcinogenesis, such as "positive regulation of cell growth" and "positive regulation of extracellular signal-regulated kinase (ERK1) and ERK2 cascade" were statistically significant (Fig. 4C). Similarly, in the genes commonly up-regulated in the induced cells and both cancer cell lines, the GO terms "canonical Wnt signaling pathway," "regulation of cell cycle process," and "cellular response to epidermal growth factor stimulus" were statistically significant (Fig. 4C). The gene cluster up-regulated in the induced cells and HuCCT1 cells were enriched in genes associated with the GO terms "positive regulation of cell division," "activation of mitogen-activated protein kinase kinase (MAPKK) activity," "regulation of ERK1 and ERK2 cascade," and "positive regulation of cell proliferation" (Fig. 4C). Taken together, these results demonstrated that genes associated with carcinogenesis and proliferation were up-regulated in the induced cells, as in human cancer cell lines.

Next, we sought to compare the induced cells with clinical liver cancer tissues. To this end, we performed gene set enrichment analysis using gene sets up-regulated in clinical liver cancer[35] and in normal liver tissues.[36] The data showed that the genes up-regulated in HCC compared to normal liver samples were highly enriched in the induced cells, similar to HepG2 cells. Conversely, liver-specific genes were enriched in hepatocytes compared to the induced and HepG2 cells (Fig. 4D). The results indicated that the induced cells acquired gene expression patterns characteristic of clinical liver cancers and concomitantly lost hepatic functions like HepG2 cells. Simultaneously, GO analyses of down-regulated genes in the induced cells compared to HUVECs showed that the terms "angiogenesis," "sprouting angiogenesis," "positive regulation of endothelial cell migration," "positive regulation of endothelial cell proliferation," and "vasculogenesis" were statistically significant (Supporting Fig. S5A). In addition, the endothelial cell marker genes platelet/endothelial cell adhesion molecule 1 (*PECAM1*; well known as *CD31)*, *CDH5* (well known as VE-cadherin), and nitric oxide synthase 3 (*NOS3*; well known as endothelial nitric oxide synthase [eNOS]) were down-regulated in the induced cells (Supporting Fig. S5B). These results

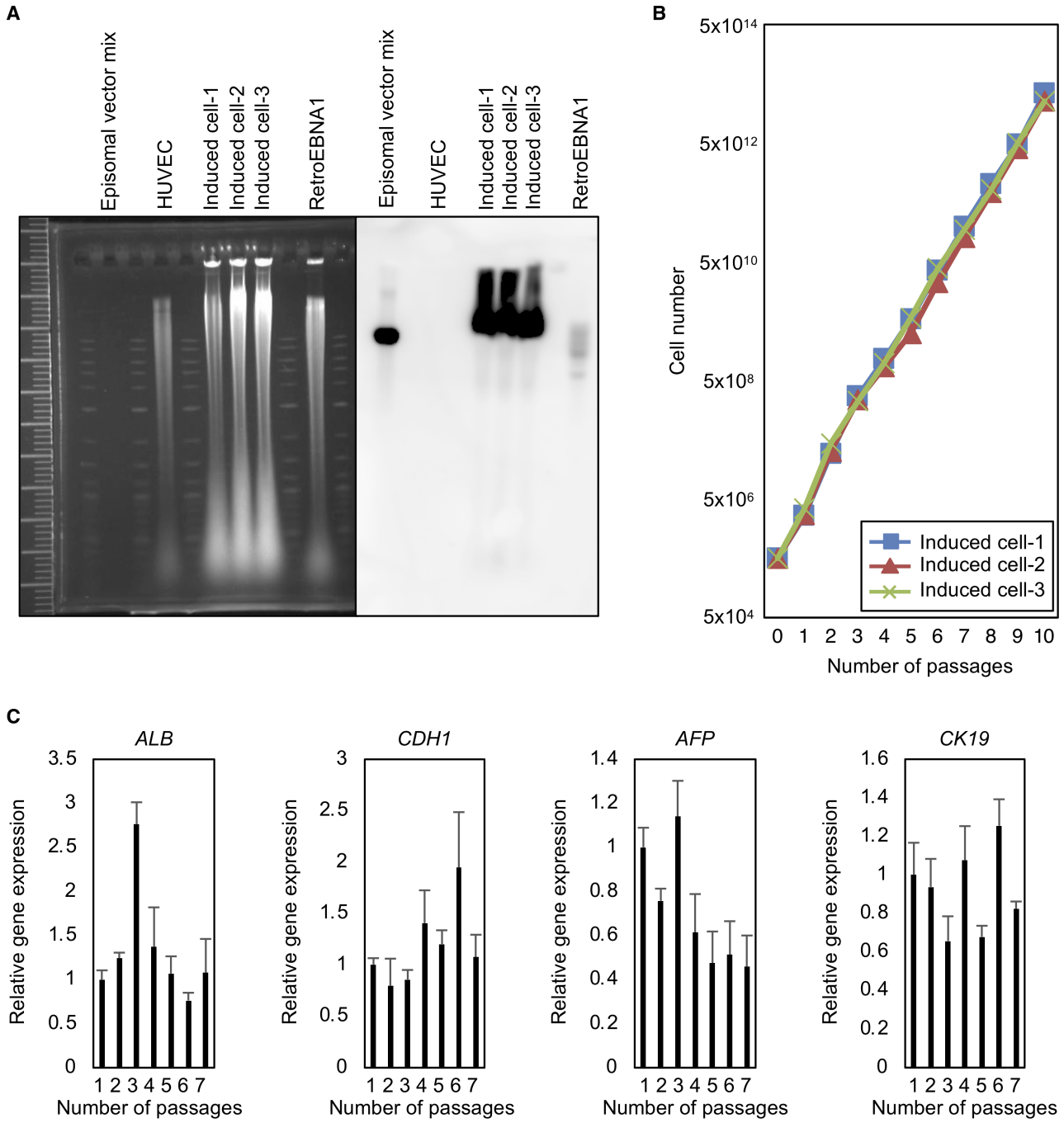

FIG. 3. Evaluation of genomic insertion and expansion in long-term culture. (A) Genomic Southern blotting of HUVECs, three different induced cells, and HUVECs infected with retroEBNA1 using an EBNA1 probe. (B) Growth curves of three different induced cells in three independent experiments. Cells were passaged every 14 days in wells of six-well plates (split ratio 1:5). (C) qPCR analyses were performed with total RNA obtained from the induced cells at the indicated passage numbers. All data were normalized with the values for induced cells at passage 1, and the fold differences are shown. Data represent the mean ± SD; n = 3 independent experiments. Abbreviation: retroEBNA1, retrovirus expressing EBNA1.

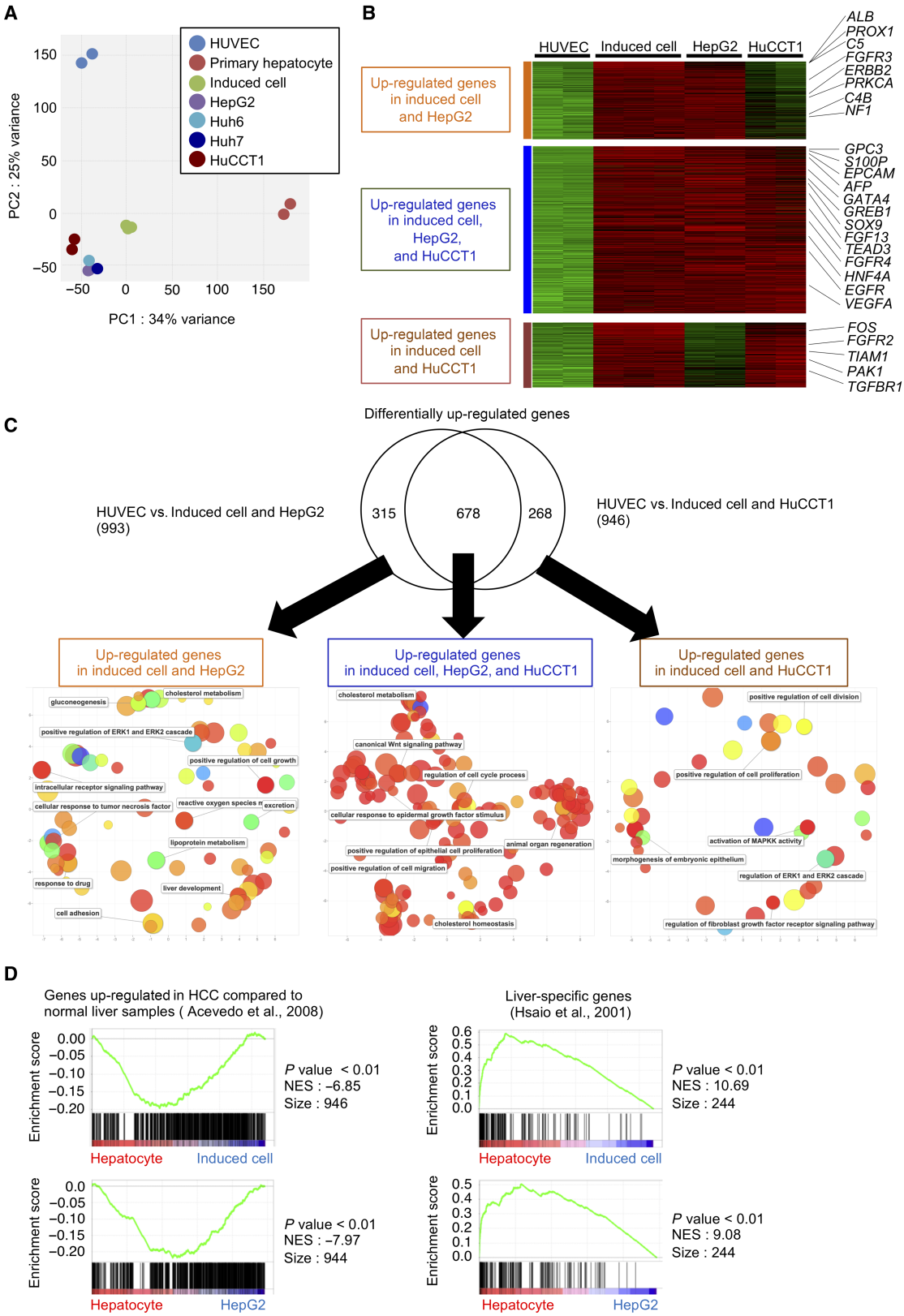
A
HUVEC
Primary hepatocyte
Induced cell
HepG2
Huh6
Huh7
HuCCT1
PC2 : 25% variance
PC1 : 34% variance
B
HUVEC
Induced cell
HepG2
HuCCT1
Up-regulated genes in induced cell and HepG2
Up-regulated genes in induced cell, HepG2, and HuCCT1
Up-regulated genes in induced cell and HuCCT1
ALB
PROX1
C5
FGFR3
ERBB2
PRKCA
C4B
NF1
GPC3
S100P
EPCAM
AFP
GATA4
GREB1
SOX9
FGF13
TEAD3
FGFR4
HNF4A
EGFR
VEGFA
FOS
FGFR2
TIAM1
PAK1
TGFBR1
C
Differentially up-regulated genes
HUVEC vs. Induced cell and HepG2 (993)
315
678
268
HUVEC vs. Induced cell and HuCCT1 (946)
Up-regulated genes in induced cell and HepG2
Up-regulated genes in induced cell, HepG2, and HuCCT1
Up-regulated genes in induced cell and HuCCT1
gluconeogenesis
cholesterol metabolism
positive regulation of ERK1 and ERK2 cascade
positive regulation of cell growth
intracellular receptor signaling pathway
cellular response to tumor necrosis factor
lipoprotein metabolism
response to drug
liver development
cell adhesion
canonical Wnt signaling pathway
regulation of cell cycle process
cellular response to epidermal growth factor stimulus
positive regulation of epithelial cell proliferation
animal organ regeneration
positive regulation of cell migration
cholesterol homeostasis
positive regulation of cell division
positive regulation of cell proliferation
activation of MAPKK activity
morphogenesis of embryonic epithelium
regulation of ERK1 and ERK2 cascade
regulation of fibroblast growth factor receptor signaling pathway
D
Genes up-regulated in HCC compared to normal liver samples (Acevedo et al., 2008)
Liver-specific genes (Hsaio et al., 2001)
Enrichment score
P value < 0.01
NES : −6.85
Size : 946
P value < 0.01
NES : 10.69
Size : 244
P value < 0.01
NES : −7.97
Size : 944
P value < 0.01
NES : 9.08
Size : 244
Hepatocyte
Induced cell
HepG2

FIG. 4. Global gene expression profiles and functional properties of induced cells. (A) Principal component analysis was performed using 3' untranslated region sequencing (CEL-seq2) data on HUVECs, human primary hepatocytes, induced cells, HepG2 cells, Huh6 cells, Huh7 cells, and HuCCT1 cells. (B) Heatmap image from CEL-seq2 data showing the differentially expressed genes in HUVECs, induced cells, HepG2 cells, and HuCCT1 cells. (C) Venn diagram showing the degree of overlap of genes up-regulated more than 8-fold in the induced cells, HepG2 cells, and HuCCT1 cells compared to HUVECs. DAVID was used to identify significantly enriched GO terms from the list of genes contained in each of the three groups of the Venn diagram. Similar GO terms were clustered semantically using REVIGO, and the data are shown as scatter plots. The color and size of circles indicate the $\log_{10}$ *P* value and frequency of the GO terms, respectively. (D) GSEA of CEL-seq2 data for induced cells, hepatocytes, and HepG2 cells was performed using gene sets for up-regulated in HCC compared to normal liver samples (gene set name, ACEVEDO_LIVER_CANCER_UP) and liver-specific genes (gene set name, HSAIO_LIVER_SPECIFIC_GENES). Abbreviations: C4B, complement C4B (Chido blood group); CEL-seq2, cell expression by linear amplification and sequencing 2; DAVID, database for annotation, visualization, and integrated discovery; EGFR, epidermal growth factor receptor; FGFR4, fibroblast growth factor receptor 4; FOS, Fos proto-oncogene, AP-1 transcription factor subunit; GREB1, growth regulating estrogen receptor binding 1; GSEA, gene set enrichment analysis; MAPKK, mitogen-activated protein kinase kinase; NES, normalized enrichment score; NF1, neurofibromin 1; PC, principal component; PRKCA, protein kinase C alpha; PROX1, prospero homeobox 1; REVIGO, reduce and visualize gene ontology; S100P, S100 calcium binding protein P; TEAD3, TEA domain transcription factor 3; VEGFA, vascular endothelial growth factor A.

demonstrated the loss of endothelial cell properties by direct reprogramming. Taken together, transcriptome analyses revealed that the induced cells were similar to both HCC and CCC.

CARCINOGENESIS OF INDUCED CELLS *IN VIVO*

Finally, we assessed whether the induced cells generated liver cancer *in vivo*. To achieve efficient engraftment of cell transplantation, we intrasplenically injected the induced cells or HUVECs into the liver of retrorsine-treated NSG mice after 70% partial hepatectomy as described.[5] Notably, all induced cells (in five independent experiments) formed liver tumors *in vivo* at 2 months after transplantation in contrast to the absence of tumors in livers transplanted with HUVECs (Fig. 5A). Transplanted induced cells formed tumors in the liver but not in other organs, suggesting that tumor metastasis did not occur in the recipient mice. Hematoxylin and eosin (H&E) staining showed that the induced cells formed multiple nodules in the remnant liver (Fig. 5B). Immunohistochemical staining showed that the tumor expressed human-specific α-1 antitrypsin (hAAT), which confirmed that the tumors were derived from the induced cells. Immunohistochemical staining of serial sections revealed that hAAT-positive tumor cells comprised Ki67-positive proliferating cells and cleaved caspase 3-positive apoptotic cells (Fig. 5C). Electron microscopic analysis showed anisonucleosis, pleiomorphic nuclei, increased nuclear-to-cytoplasmic ratio, and decreased cytoplasmic organelles in the induced cell-derived tumors. The tumor cell nuclei were irregular in shape with euchromatin, which is characteristic of human cancer cells. Bile canaliculi-like structures formed in HCC[37] were also observed in tumors derived from the induced cells (Fig. 5D). These microscopic and electron microscopic findings were consistent with the features of human liver cancer. Furthermore, the tumors expressed HCC and CCC marker genes and formed several histologic patterns in the same nodule (Fig. 5E,F). The compact type of HCC structure formed by the trabeculae growing, compressing the sinusoids, and forming sheets of tumor cells was seen in a compartment of a tumor nodule. Another compartment was formed by the HCC pseudoglandular-type-like structure, which was characterized by gland-like spaces lined by tumor cells. Notably, the tumors also contained a CCC-like compartment with mucin production. These features are characteristic of the intermediate-cell subtype of human combined hepatocellular–cholangiocarcinoma (CHC). In addition, F4/80-positive Kupffer cells/macrophages and CD31-positive endothelial cells infiltrated the tumors (Fig. 5G), suggesting that the tumor microenvironment generated in the induced cell-derived tumors is similar to that formed in human liver cancer. Finally, we compared the induced cell-derived tumors and human liver cancers transcriptomically. To avoid inaccurate gene expression estimates by the contamination of host mouse transcripts, we used bamcmp,[38] an algorithm aiming to distinguish between the human-derived and host mouse-derived sequence reads. After data processing with bamcmp, we compared the global gene expression profile of induced cell-derived tumors and that from published data of HCC (GSE69164), CCC (GSE63420), and normal liver tissues (GSE112221). This analysis demonstrated that many genes associated with liver

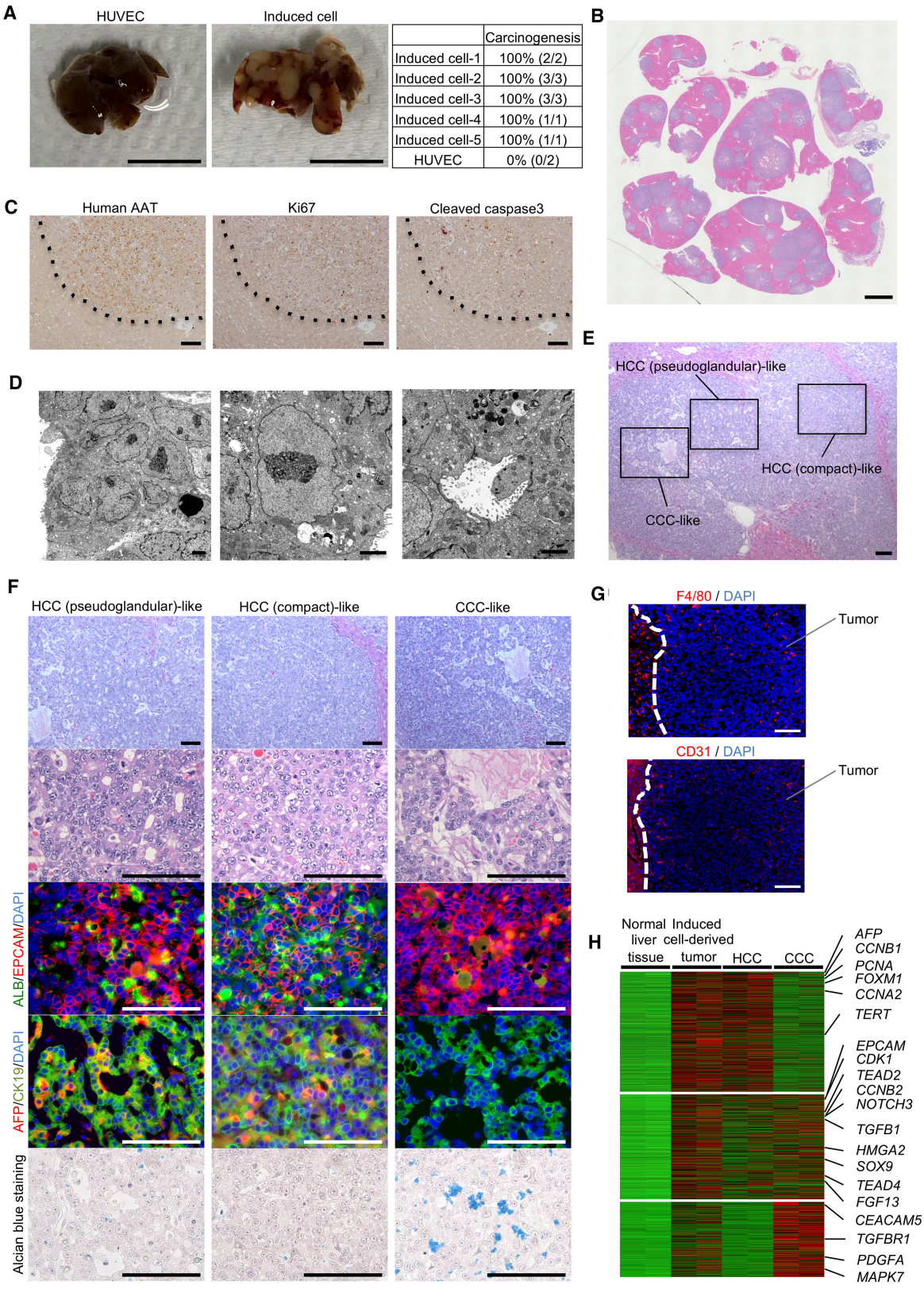
A
HUVEC
Induced cell
Carcinogenesis
Induced cell-1 100% (2/2)
Induced cell-2 100% (3/3)
Induced cell-3 100% (3/3)
Induced cell-4 100% (1/1)
Induced cell-5 100% (1/1)
HUVEC 0% (0/2)
B
C
Human AAT
Ki67
Cleaved caspase3
D
E
HCC (pseudoglandular)-like
HCC (compact)-like
CCC-like
F
HCC (pseudoglandular)-like
HCC (compact)-like
CCC-like
ALB/EPCAM/DAPI
AFP/CK19/DAPI
Alcian blue staining
G
F4/80 / DAPI
Tumor
CD31 / DAPI
Tumor
H
Normal liver tissue
Induced cell-derived tumor
HCC
CCC
AFP
CCNB1
PCNA
FOXM1
CCNA2
TERT
EPCAM
CDK1
TEAD2
CCNB2
NOTCH3
TGFB1
HMGA2
SOX9
TEAD4
FGF13
CEACAM5
TGFBR1
PDGFA
MAPK7

FIG. 5. Induced cells formed liver tumors *in vivo*. (A) Representative gross pathology of an HUVEC-transplanted liver and an induced cell-transplanted liver. Scale bars, 10 mm. Table on the right shows the percentage of tumors. The numbers in parentheses denote the number of experiments. (B) Low-magnification image of an H&E-stained section obtained from an induced cell-transplanted liver. Scale bar, 2 mm. (C) Immunohistochemical staining of hAAT, Ki67, and cleaved caspase 3 in a liver tumor derived from induced cells. Scale bars, 100 μm. (D) Representative ultrastructural images of liver tumors derived from induced cells. Scale bars, 2 μm. (E,F) Representative images of H&E-stained liver tumor, HCC (pseudoglandular)-like area, HCC (compact)-like area, and CCC-like area (right). Co-immunofluorescent staining of ALB with EPCAM and that of AFP with CK19 in each area. Alcian blue staining was also conducted for each area. DNA was stained with DAPI. Scale bars, 100 μm. (G) Immunofluorescent staining of F4/80 (upper panel) and CD31 (lower panel) in liver tumors derived from induced cells. DNA was stained with DAPI. Scale bars, 100 μm. (H) Heatmap image from RNA sequencing data shows the differentially expressed genes in induced cell-derived tumors, HCC, and CCC compared to those in normal liver tissue. The tissue sections displayed in Fig. 5 were obtained from a representative recipient mouse, and other recipient mice showed similar histologic characteristics. Abbreviations: FOXM1, forkhead box M1; MAPK7, mitogen-activated protein kinase 7; PDGFA, platelet derived growth factor subunit A.

cancer were commonly up-regulated in the induced cell-derived tumors and human liver cancers (Fig. 5H). Similar to the induced cells *in vitro*, the HCC-specific gene *AFP*, the immature cell marker genes *EPCAM* and *SOX9*, and *FGF13* associated with FGF signaling were up-regulated in the induced cell-derived tumors. Moreover, telomerase reverse transcriptase (*TERT*), which has a promoter that is frequently mutated in HCC[3]; cell cycle-related genes (cyclin A2 [*CCNA2*], *CCNB1*, *CCNB2*, cyclin dependent kinase 1 [*CDK1*], and proliferating cell nuclear antigen [*PCNA*]); TEA domain transcription factor 2 [*TEAD2*] and *TEAD4* involved in the Hippo pathway, which is related to liver carcinogenesis[4]; transforming growth factor beta 1 (*TGFB1*) and *TGFBR1*, which are activated in HCC proliferation subclass[3]; notch receptor 3 (*NOTCH3*), which is associated with NOTCH signaling involved in liver carcinogenesis[4]; and the CCC marker gene CEA cell adhesion molecule 5 (*CEACAM5*)[39] were up-regulated in the induced cell-derived tumors. Taken together, the induced cell-derived tumors transcriptomically resembled human liver cancer. In conclusion, we succeeded in generating iLCCs capable of developing into human liver cancer-like tumors *in vivo*.

Discussion

In this study, using nonintegrative episomal vectors, we generated HUVEC-derived iLCCs that exhibited properties of human clinical liver cancers *in vitro* and *in vivo*. To incorporate malignant capacity, we selected the oncogene, *LIN28B*. *LIN28B* up-regulates *let-7* targeted genes by inhibiting *let-7* maturation. *Let-7* targets several oncogenes, such as *RAS*, *MYC*, high mobility group AT-hook 2 (*HMGA2*), and PR domain containing 1, with ZNF domain (*BLIMP1*), and cell cycle-associated genes, such as *CCND1* and *CCND2*. In fact, *LIN28A/B* expression and *let-7* loss have been reported to correlate with poor prognosis in several cancers.[40] Furthermore, genetically modified mouse models with overexpression of *Lin28a/b* alone resulted in liver cancer,[13] intestinal cancer,[41,42] Wilms tumor,[43] peripheral T-cell lymphoma,[44] and neuroblastoma.[45] These reports indicated that the robust oncogenic capacity of *LIN28B* was associated with cancer initiation and progression in several cancers. In human liver cancer as well, *LIN28B* has been associated with poor prognosis[46] and is likely related to initiation and progression. LIN28B may also play a key role in hepatic lineage commitment during development. Our previous report demonstrated that *Lin28b* is specifically expressed in mouse hepatoblasts and maintains their stem cell properties during development.[14] Our present data showed that *LIN28B* withdrawal decreased the expression of *ALB* and *CDH1* in our candidate gene-screening experiment. Thus, LIN28B could be considered a key factor not only in the acquisition of cancerous properties but also in the induction of immature hepatic phenotype.

Recent integrative analyses have demonstrated that clinical liver cancer accumulates multiple oncogenic mutations.[3] Recapitulation of these driver mutations is a promising approach to generate liver cancer models. However, complete recapitulation is practically challenging because clinical liver cancers accumulate several mutations simultaneously and because inter-patient, intertumoral, and intratumoral heterogeneities exist. In this study, we attempted to influence the expression of several driver genes by overexpression of *LIN28B* instead of recapitulating driver mutations.

This strategy, involving modification of factors that have regulatory capacities of oncogenes, is a novel and promising approach for research on cancer initiation, progression, and therapy. Moreover, in contrast to the two-step reprogramming method for cancer organoids,[8] we developed a simple one-step method for generating human liver cancer cells. This simple method may have advantages in cost, time, and reproducibility. Especially, a high reproducibility of tumor formation by transplanted induced cells may be favorable for cancer research.

Under three-dimensional culture conditions, iLCCs formed organoids that have cancerous properties, such as increased nucleus-to-cytoplasm ratio and enlarged pleomorphic nuclei. However, iLCCs did not show anchorage-independent growth ability in a soft-agar colony formation assay. Although the anchorage-independent growth correlates with tumorigenicity of cancer cell lines, it was reported that not all primary cancer cells showed the anchorage-independent growth.[47] Thus, it is suggested that the lack of anchorage-independent growth potential in iLCCs does not remove the possibility of cancerous characteristics and that iLCCs have a low grade of malignancy in culture. Furthermore, a part of iLCCs showed chromosomal instability in culture, which is often observed in liver cancers.[3] These findings raise the possibility that iLCCs *in vitro* reach the state of cancer cells and be applicable to *in vitro* analysis for cancer research. In future studies, we should investigate the availability of iLCCs *in vitro* for cancer research, such as drug screening.

Histologically, the iLCC-derived tumors closely resembled those of human CHCs. This is in contrast with HCC- or hepatoblastoma-like tumors that were previously reported in *Lin28b*-overexpressing mouse liver.[13] In other genetically modified models, CHC-like tumors have been reported.[5] Tumor phenotypes may depend on the differentiation stage of the initial cells. iLCCs are possibly more immature and malignant than *lin28b*-overexpressing hepatocytes. As *KLF5* has been reported to be associated with cancer stem cells,[48] it may play an important role in the formation of a CHC-like phenotype through an immature state.

In clinical settings, HCC and CCC are treated as independent diseases and the therapeutic strategies differ vastly. However, a recent integrative analysis showed that the HCC subtype that exhibited CCC-like gene expression patterns was more aggressive and associated with poor prognosis.[49] CCC-like HCCs have also been reported to express stem cell-like traits. Similarly, the aggressive subtype in CCC displayed gene expression patterns similar to those of an aggressive subtype of HCC.[50] These reports indicate that the overlap between HCC and CCC is associated with aggressive subtypes, poor prognosis, and stem cell features. These aggressive subtypes of HCC/CCC and CHC may be derived from a common precursor with stem cell features, and the similarities between these tumors may be greater than previously known. Our data suggest that the iLCCs mimic liver cancer with stem cell-like features and may thus contribute to future research, especially on aggressive subtypes of liver cancers.

Recently, molecular-targeted drugs have been used in the clinical treatment of HCC. However, no standard therapy using molecular-targeted drugs has been established for CCC and CHC. As CHC is a rare cancer, there is no standard treatment for CHC. iLCCs may facilitate drug development and therapeutic strategies for liver cancer with stem cell features. In fact, multikinase inhibitors, such as sorafenib, lenvatinib, and regorafenib, have been used for HCC treatment, and *FGFR*, one of the targets of these multikinase inhibitors, was up-regulated in iLCCs.

It remains unclear whether other cell types can be reprogrammed to iLCCs. In our future studies, we should examine whether we can use the one-step iLCC induction method for cells obtained from patients with cancer. Human peripheral blood-derived endothelial cells (HPBECs) may be a candidate source of iLCCs because HPBECs resemble HUVECs and achieved reprogramming to iHepPCs.[5] Also, we expect that iLCCs can be generated from human peripheral blood mononuclear cells, which may be more suitable for clinical applications.

Taken together, the iLCCs generated using our method may provide a novel tool for basic science research and potential therapies for aggressive liver cancer with stem cell features.

Acknowledgment: We thank Drs. Masafumi Onodera, Hiroyuki Miyoshi, Sinya Yamanaka, and Jin-Tang Dong for sharing reagents and Yuuki Honda, Mariko Tasai, Chiaki Kaieda, Kanako Ichikawa, Ryo Ugawa, and Emiko Koba for their excellent technical assistance.

REFERENCES

1) Villanueva A. Hepatocellular carcinoma. N Engl J Med 2019;380:1450-1462.
2) Heindryckx F, Colle I, Van Vlierberghe H. Experimental mouse models for hepatocellular carcinoma research. Int J Exp Pathol 2009;90:367-386.
3) Zucman-Rossi J, Villanueva A, Nault JC, Llovet JM. Genetic landscape and biomarkers of hepatocellular carcinoma. Gastroenterology 2015;149:1226-1239.e4.
4) Sia D, Villanueva A, Friedman SL, Llovet JM. Liver cancer cell of origin, molecular class, and effects on patient prognosis. Gastroenterology 2017;152:745-761.
5) **Inada H**, **Udono M**, Matsuda-Ito K, Horisawa K, Ohkawa Y, Miura S, et al. Direct reprogramming of human umbilical vein- and peripheral blood-derived endothelial cells into hepatic progenitor cells. Nat Commun 2020;11:5292.
6) Takahashi K, Yamanaka S. Induction of pluripotent stem cells from mouse embryonic and adult fibroblast cultures by defined factors. Cell 2006;126:663-676.
7) **Zhao Y**, **Yin X**, **Qin H**, Zhu F, Liu H, Yang W, et al. Two supporting factors greatly improve the efficiency of human iPSC generation. Cell Stem Cell 2008;3:475-479.
8) **Sun L**, **Wang Y**, Cen J, Ma X, Cui L, Qiu Z, et al. Modelling liver cancer initiation with organoids derived from directly reprogrammed human hepatocytes. Nat Cell Biol 2019;21:1015-1026.
9) Okita K, Yamakawa T, Matsumura Y, Sato Y, Amano N, Watanabe A, et al. An efficient nonviral method to generate integration-free human-induced pluripotent stem cells from cord blood and peripheral blood cells. Stem Cells 2013;31:458-466.
10) **Sung W-K**, **Zheng H**, **Li S**, **Chen R**, **Liu X**, Li Y, et al. Genome-wide survey of recurrent HBV integration in hepatocellular carcinoma. Nat Genet 2012;44:765-769.
11) **Nault J-C**, **Datta S**, **Imbeaud S**, Franconi A, Mallet M, Couchy G, et al. Recurrent AAV2-related insertional mutagenesis in human hepatocellular carcinomas. Nat Genet 2015;47:1187-1193.
12) Hacein-Bey-Abina S, von Kalle C, Schmidt M, Le Deist F, Wulffraat N, McIntyre E, et al. A serious adverse event after successful gene therapy for X-linked severe combined immunodeficiency. N Engl J Med 2003;348:255-256.
13) **Nguyen L**, **Robinton D**, **Seligson M**, Wu L, Li L, Rakheja D, et al. Lin28b is sufficient to drive liver cancer and necessary for its maintenance in murine models. Cancer Cell 2014;26:248-261.
14) Takashima Y, Terada M, Udono M, Miura S, Yamamoto J, Suzuki A. Suppression of lethal-7b and miR-125a/b maturation by Lin28b enables maintenance of stem cell properties in hepatoblasts. Hepatology 2016;64:245-260.
15) Thorgeirsson SS, Santoni-Rugiu E. Transgenic mouse models in carcinogenesis: interaction of c-myc with transforming growth factor and hepatocyte growth factor in hepatocarcinogenesis. Br J Clin Pharmacol 1996;42:43-52.
16) Manier S, Powers JT, Sacco A, Glavey SV, Huynh D, Reagan MR, et al. The LIN28B/let-7 axis is a novel therapeutic pathway in multiple myeloma. Leukemia 2017;31:853-860.
17) Chang T-C, Zeitels LR, Hwang H-W, Chivukula RR, Wentzel EA, Dews M, et al. Lin-28B transactivation is necessary for Myc-mediated let-7 repression and proliferation. Proc Natl Acad Sci U S A 2009;106:3384-3389.
18) An T, Dong T, Zhou H, Chen Y, Zhang J, Zhang YU, et al. The transcription factor Krüppel-like factor 5 promotes cell growth and metastasis via activating PI3K/AKT/Snail signaling in hepatocellular carcinoma. Biochem Biophys Res Commun 2019;508:159-168.
19) Honda K, Sbisà E, Tullo A, Papeo PA, Saccone C, Poole S, et al. P53 mutation is a poor prognostic indicator for survival in patients with hepatocellular carcinoma undergoing surgical tumour ablation. Br J Cancer 1998;77:776-782.
20) Miura S, Suzuki A. Generation of mouse and human organoid-forming intestinal progenitor cells by direct reprogramming. Cell Stem Cell 2017;21:456-471.e5.
21) **Wen W**, **Zhang J-P**, **Xu J**, Su RJ, Neises A, Ji G-Z, et al. Enhanced generation of integration-free iPSCs from human adult peripheral blood mononuclear cells with an optimal combination of episomal vectors. Stem Cell Reports 2016;6:873-884.
22) Qiu WH, Zhou BS, Chu PG, Chen WG, Chung C, Shih J, et al. Over-expression of fibroblast growth factor receptor 3 in human hepatocellular carcinoma. World J Gastroenterol 2005;11:5266-5272.
23) Liu J, Ahiekpor A, Li L, Li X, Arbuthnot P, Kew M, et al. Increased expression of ErbB-2 in liver is associated with hepatitis B x antigen and shorter survival in patients with liver cancer. Int J Cancer 2009;125:1894-1901.
24) Nakatsura T, Yoshitake Y, Senju S, Monji M, Komori H, Motomura Y, et al. Glypican-3, overexpressed specifically in human hepatocellular carcinoma, is a novel tumor marker. Biochem Biophys Res Commun 2003;306:16-25.
25) Yamashita T, Forgues M, Wang W, Kim JW, Ye Q, Jia H, et al. EpCAM and α-fetoprotein expression defines novel prognostic subtypes of hepatocellular carcinoma. Cancer Res 2008;68:1451-1461.
26) **Guo X**, **Xiong LU**, Sun T, Peng R, Zou L, Zhu H, et al. Expression features of SOX9 associate with tumor progression and poor prognosis of hepatocellular carcinoma. Diagn Pathol 2012;7:44.
27) Matsushima H, Kuroki T, Kitasato A, Adachi T, Tanaka T, Hirabaru M, et al. Sox9 expression in carcinogenesis and its clinical significance in intrahepatic cholangiocarcinoma. Dig Liver Dis 2015;47:1067-1075.
28) Sulpice L, Rayar M, Turlin B, Boucher E, Bellaud P, Desille M, et al. Epithelial cell adhesion molecule is a prognosis marker for intrahepatic cholangiocarcinoma. J Surg Res 2014;192:117-123.
29) Motoo Y, Sawabu N, Nakanuma Y. Expression of epidermal growth factor and fibroblast growth factor in human hepatocellular carcinoma: an immunohistochemical study. Liver 1991;11:272-277.
30) Harimoto N, Taguchi K, Shirabe K, Adachi E, Sakaguchi Y, Toh Y, et al. The significance of fibroblast growth factor receptor 2 expression in differentiation of hepatocellular carcinoma. Oncology 2010;78:361-368.
31) **Arai Y**, **Totoki Y**, **Hosoda F**, Shirota T, Hama N, Nakamura H, et al. Fibroblast growth factor receptor 2 tyrosine kinase fusions define a unique molecular subtype of cholangiocarcinoma. Hepatology 2014;59:1427-1434.
32) Clapéron A, Mergey M, Nguyen Ho-Bouldoires TH, Vignjevic D, Wendum D, Chrétien Y, et al. EGF/EGFR axis contributes to the progression of cholangiocarcinoma through the induction of an epithelial-mesenchymal transition. J Hepatol 2014;61:325-332.
33) **Ding Y**, **Chen B**, Wang S, Zhao L, Chen J, Ding Y, et al. Overexpression of Tiaml in hepatocellular carcinomas predicts poor prognosis of HCC patients. Int J Cancer 2009;124:653-658.
34) Ching YP, Leong VYL, Lee MF, Xu HT, Jin DY, Ng IOL. P21-activated protein kinase is overexpressed in hepatocellular carcinoma and enhances cancer metastasis involving c-Jun NH2-terminal kinase activation and paxillin phosphorylation. Cancer Res 2007;67:3601-3608.
35) Acevedo LG, Bieda M, Green R, Farnham PJ. Analysis of the mechanisms mediating tumor-specific changes in gene expression in human liver tumors. Cancer Res 2008;68:2641-2651.
36) Hsiao L-L, Dangond F, Yoshida T, Hong R, Jensen RV, Misra J, et al. A compendium of gene expression in normal human tissues. Physiol Genomics 2001;7:97-104.

37) Isomura T, Nakashima T. Ultrastructure of human hepatocellular carcinoma. Acta Pathol Jpn 1980;30:713-726.
38) Khandelwal G, Girotti MR, Smowton C, Taylor S, Wirth C, Dynowski M, et al. Next-generation sequencing analysis and algorithms for PDX and CDX models. Mol Cancer Res 2017;15:1012-1016.
39) Subrungruanga I, Thawornkunob C, Chawalitchewinkoon-Petmitrc P, Pairojkul C, Wongkham S, Petmitrb S, et al. Gene expression profiling of intrahepatic cholangiocarcinoma. Asian Pac J Cancer Prev 2013;14:557-563.
40) **Balzeau J**, **Menezes MR**, **Cao S**, Hagan JP. The LIN28/let-7 pathway in cancer. Front Genet 2017;8:31.
41) Madison BB, Liu QI, Zhong X, Hahn CM, Lin N, Emmett MJ, et al. LIN28B promotes growth and tumorigenesis of the intestinal epithelium via Let-7. Genes Dev 2013;27:2233-2245.
42) Tu H-C, Schwitalla S, Qian Z, LaPier GS, Yermalovich A, Ku Y-C, et al. LIN28 cooperates with WNT signaling to drive invasive intestinal and colorectal adenocarcinoma in mice and humans. Genes Dev 2015;29:1074-1086.
43) Urbach A, Yermalovich A, Zhang J, Spina CS, Zhu H, Perez-Atayde AR, et al. Lin28 sustains early renal progenitors and induces Wilms tumor. Genes Dev 2014;28:971-982.
44) Beachy SH, Onozawa M, Chung YJ, Slape C, Bilke S, Francis P, et al. Enforced expression of Lin28b leads to impaired T-cell development, release of inflammatory cytokines, and peripheral T-cell lymphoma. Blood 2012;120:1048-1059.
45) Molenaar JJ, Domingo-Fernández R, Ebus ME, Lindner S, Koster J, Drabek K, et al. LIN28B induces neuroblastoma and enhances MYCN levels via let-7 suppression. Nat Genet 2012;44:1199-1206.
46) Viswanathan SR, Powers JT, Einhorn W, Hoshida Y, Ng TL, Toffanin S, et al. Lin28 promotes transformation and is associated with advanced human malignancies. Nat Genet 2009;41:843-848.
47) Nomura Y, Tashiro H, Hisamatsu K. *In vitro* clonogenic growth and metastatic potential of human operable breast cancer. Cancer Res 1989;49:5288-5293.
48) **Maehara O**, **Sato F**, Natsuizaka M, Asano A, Kubota Y, Itoh J, et al. A pivotal role of Krüppel-like factor 5 in regulation of cancer stem-like cells in hepatocellular carcinoma. Cancer Biol Ther 2015;16:1453-1461.
49) Woo HG, Lee J-H, Yoon J-H, Kim CY, Lee H-S, Jang JJ, et al. Identification of a cholangiocarcinoma-like gene expression trait in hepatocellular carcinoma. Cancer Res 2010;70:3034-3041.
50) Sia D, Hoshida Y, Villanueva A, Roayaie S, Ferrer J, Tabak B, et al. Integrative molecular analysis of intrahepatic cholangiocarcinoma reveals 2 classes that have different outcomes. Gastroenterology 2013;144:829-840.

Author names in bold designate shared co-first authorship.

Supporting Information

Additional Supporting Information may be found at onlinelibrary.wiley.com/doi/10.1002/hep4.1911/suppinfo.